Available online at www.sciencedirect.com
ScienceDirect
International Journal of Multiphase Flow 32 (2006) 1340–1353
International Journal of Multiphase Flow
www.elsevier.com/locate/ijmulflow

Two-phase flow distribution of air–water annular flow in a parallel flow heat exchanger

Nae-Hyun Kim *, Tae-Ryong Sin

Department of Mechanical Engineering, University of Incheon, 177 Dohwa-Dong, Nam-Gu, Incheon 402-749, Republic of Korea

Received 28 November 2005; received in revised form 11 July 2006

Abstract

The air and water flow distribution are experimentally studied for a round header – flat tube geometry simulating a parallel flow heat exchanger. The number of branch flat tube is 30. The effects of tube outlet direction, tube protrusion depth as well as mass flux, and quality are investigated. The flow at the header inlet is identified as annular. For the downward flow configuration, the water flow distribution is significantly affected by the tube protrusion depth. For flush-mounted configuration, most of the water flows through frontal part of the header. As the protrusion depth increases, more water is forced to the rear part of the header. The effect of mass flux or quality is qualitatively the same as that of the protrusion depth. Increase of the mass flux or quality forces the water to rear part of the header. For the upward flow configuration, however, most of the water flows through rear part of the header. The protrusion depth, mass flux, or quality does not significantly alter the flow pattern. Possible explanations are provided based on the flow visualization results. Negligible difference on the water flow distribution was observed between the parallel and the reverse flow configuration.

Keywords: Flow distribution; Parallel flow heat exchanger; Air–water flow; Two-phase; Protrusion

1. Introduction

Brazed aluminum heat exchangers consist of flat tubes of 1–2 mm hydraulic diameter on the refrigerant-side, and louver fins on the air-side. They are seriously considered as evaporators of residential air conditioners due to the superior thermal performance as compared with conventional fin-tube heat exchangers. To manage the excessive tube-side pressure drop by small channel size, a number of tubes are grouped to one pass using a header (parallel flow configuration). To use the parallel flow heat exchanger as a refrigerant evaporator, it is very important to evenly distribute the two-phase refrigerant (especially the liquid) into the tubes. Otherwise, the thermal performance is significantly deteriorated. According to Bullard (2002), the performance reduction by flow mal-distribution could be as large as 30%. For evaporator usage, the flat tubes are installed vertically (with headers in horizontal position) to facilitate the air-side condensate drainage.

* Corresponding author. Tel.: +82 32 770 8420; fax: +82 32 770 8410.
E-mail address: knh0001@incheon.ac.kr (N.-H. Kim).

0301-9322/$ - see front matter
doi:10.1016/j.ijmultiphaseflow.2006.07.005

There are several options on the refrigerant-side design. Fig. 1 illustrates the four possible refrigerant circuits. The refrigerant may be supplied to the top header (downward flow), or they may be supplied to the bottom header (upward flow). The inlet and the exit may be located at the same side of the heat exchanger (reverse flow), or they may be located at the opposite side of the heat exchanger (parallel flow). The tube protrusion depth into the header will also affect the flow distribution. Webb and Chung (2004), Hrnjak (2004) provide recent reviews on this subject.

Watanabe et al. (1995) conducted a flow distribution study for a round header (20 mm ID) – four round tube (6 mm ID) upward flow configuration using R-11. The mass flux (based on the header cross sectional area) was varied from 40 to 120 kg/m^2 s, and the inlet quality was varied up to 0.4. The flow in the header inlet was mostly stratified. The flow distribution was highly dependent on the mass flux and the quality. Tompkins et al. (2002) tested a rectangular header – fifteen flat tube downward flow configuration using air–water. The mass flux was varied from 50 to 400 kg/m^2 s, and the quality was varied up to 0.4. The flow in the header inlet was stratified at low mass fluxes, and it was annular at high mass fluxes. The flow distribution was highly dependent on the mass flux and the quality. Better distribution was obtained at a lower mass flux (stratified flow regime). Vist and Pettersen (2004) investigated a round header (8 mm and 16 mm ID) – ten round tube (4 mm ID) configuration using R-134a. Both upward and downward flow were tested. The mass flux (based on the branch tube) was varied from 124 to 836 kg/m^2 s, and the quality was varied up to 0.5. The flow in the header inlet was mostly intermittent with some annular at high mass fluxes. For the downward flow configuration, most of the liquid flowed through frontal part of the header. For the upward configuration, on the contrary, most of the liquid flowed at the rear part of the header. The liquid distribution improved as the vapor quality decreased. The mass flux had negligible effect on the flow distribution. Lee and Lee (2004) investigated the effect of the tube protrusion depth for a vertical rectangular header (24 by 24 mm) – five horizontal rectangular branch tube configuration using air–water. The flow in the header inlet was annular. The flow distribution was highly dependent on the protrusion depth. As the protrusion depth increased, more water flowed through the downstream part of the header. Cho et al. (2003) investigated the effect of the header orientation (vertical and horizontal) and the refrigerant inlet pipe direction (inline, cross, parallel) for a round header – fifteen flat tube configuration using R-22. The mass flux was fixed at 60 kg/m^2 s, and the quality was varied up to 0.3. For the vertical header configuration, most of the liquid flowed through the frontal part of the header, and the effect of the inlet pipe direction was not significant. For a horizontal header, the flow distribution was highly dependent on the inlet pipe direction, and better distribution was obtained for the parallel or the cross flow configuration. Rong et al. (1995), Bernoux et al. (2001) provide flow distribution data for a plate heat exchanger geometry.

The literature survey reveals that the two-phase flow distribution in a header – branch tube configuration is very complex. Many parameters, both geometric and flow, affect the results, and definitely more data are needed on this subject. Especially, the effects of the tube outlet direction or the protrusion depth for a horizontal header configuration have not been investigated. In this study, the air–water flow distribution in a parallel flow heat exchanger comprised of horizontal round header (inner diameter, $D = 17$ mm) and 30 vertical flat tubes (hydraulic diameter, $D_h = 1.32$ mm) was experimentally investigated. The mass flux (based on header cross section) and the quality were varied for $70 \leqslant G \leqslant 130$ kg/m^2 s and $0.2 \leqslant x \leqslant 0.6$. The flow in the header inlet was annular. The effects of the flow direction (upward or downward), tube outlet direction

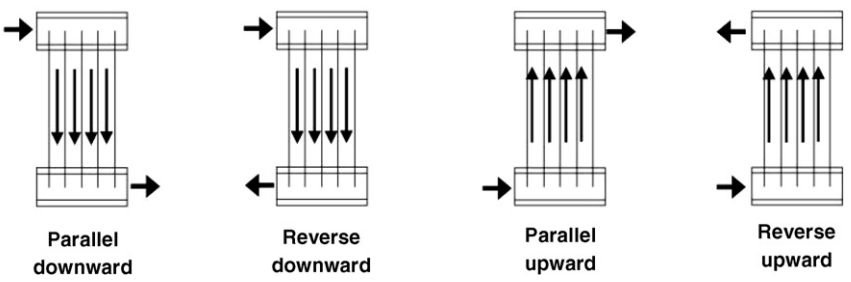

Fig. 1. Four different methods of flow distribution.

(reverse or parallel), and the tube protrusion depth (non-dimensional protrusion depth, $h/D = 0.0, 0.25, 0.5$) were systematically investigated for the mass flux and quality range.

2. Experimental apparatus

A schematic drawing of the experimental apparatus is shown in Fig. 2. The test section consists of the 17 mm ID upper and lower headers, which are 91 cm apart, and 30 flat tubes inserted at 9.8 mm pitches. This configuration was chosen to simulate the actual parallel flow heat exchanger. The cross section of the present flat tube is shown in Fig. 3. The hydraulic diameter is 1.32 mm, and the flow cross sectional area is 12.24 mm. The headers were made of transparent PVC for flow visualization. A 17 mm hole was machined longitudinally in a square PVC rod (25 mm × 25 mm × 400 mm), and 30 flat holes for insertion of flat tubes were machined at the bottom. An aluminum plate, which had matching flat holes, was installed underneath the header as illustrated in Fig. 4. Flat tubes were secured, and the protrusion depth was adjusted using O-rings between the header and the aluminum plate. Transition blocks were installed in the test section to connect the flat tubes and the 6.0 mm ID round tubes. The round tubes served as flow measurement lines. At the inlet of the header, 1.0 m long copper tube having the same inner diameter as the header was attached. The tube served as the flow development section.

The water and air, whose flow rates are separately determined, are mixed in a mixer before the air–water mixture is introduced into the header. The flow rate of every other flat tube is measured by directing the air–water mixture to the separator in the flow measurement section. As seen in Fig. 2, two valves – one at main stream, the other at by-pass stream – are installed at every other channel. Normally, main stream valves are open, and by-pass stream valves are closed. To measure the flow rate at a certain channel, the mainstream valve of the channel is closed, and the by-pass valve is open. The flow measurement principle is illustrated in Fig. 5. To prevent possible flow pattern change before and during the measurement, the differential pressure between the inlet of the upper header and the transition section was maintained the same by controlling the valve in the transition section. The pressure fluctuations during measurement were within 2% of the average value. The total water and air flow rates to the header were measured by a mass flow meter (accuracy: $\pm 1.5 \times 10^{-6}$ kg/s) and a float type flow mater (accuracy: ±1%), respectively. The tube air flow rate out of the separator was measured by a float type flow meter (accuracy: ±1%), and the tube water flow rate out of the separator was measured by weighing the drained water in a graduated cylinder. During the whole series

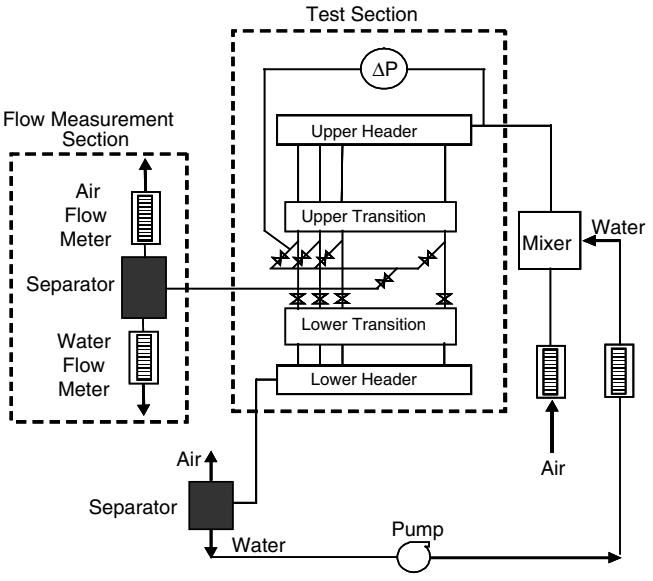

Fig. 2. Schematic drawing of the apparatus.

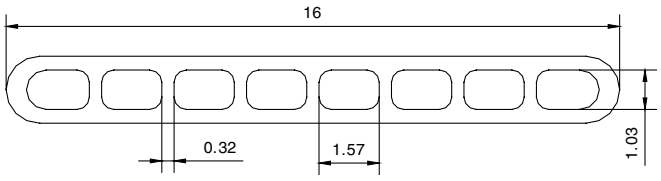

Fig. 3. Cross sectional view of the flat tube used in this study (unit: mm).

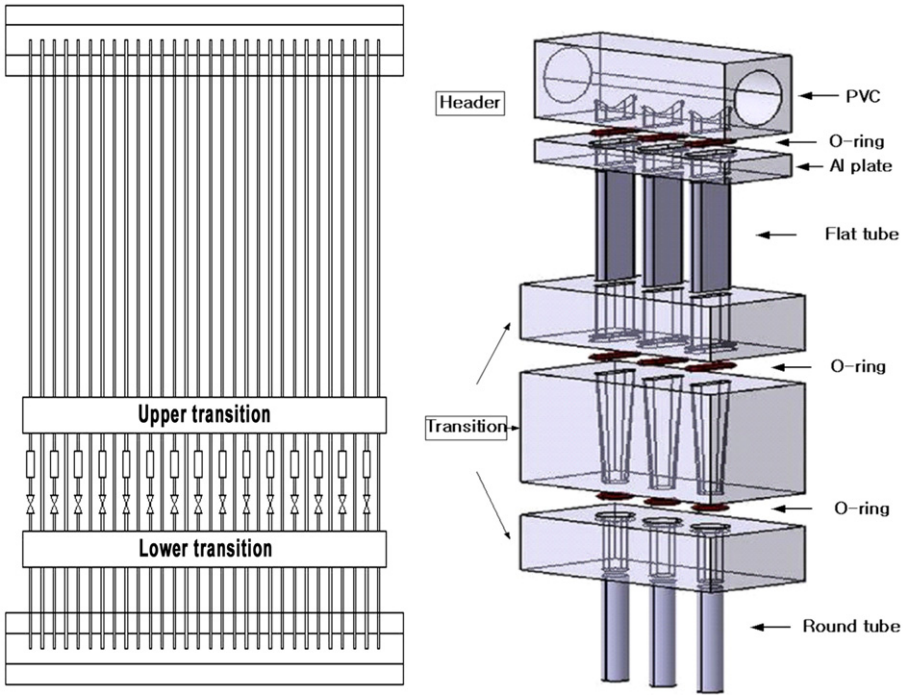

Fig. 4. Detailed drawing of the test section.

of tests, several runs were made to check the repeatability of the data. The data were repeatable within ±10%. The maximum experimental uncertainty was ±10% for the water flow rate measurement, and ±5% for the air flow rate measurement.

3. Results and discussion

3.1. Downward flow

3.1.1. Flow pattern and effect of tube protrusion depth

Typical flow pattern is illustrated in Fig. 6 along with the water and air distribution data. The ordinate of the figure is the ratio of the water or air flow rate in each tube to the average values. For flush-mounted configuration ($h/D = 0$), most of the water flows into the tubes at frontal part of the header. The data taken at $G = 100$ kg/m^2 s, $x = 0.4$ show that water flow ratio is 7.9 for the first tube, and then drastically decreases to one at fifth tube. Almost no water flows from the twenty-first tube. Although the water flow ratio changed somewhat depending on the mass flux and quality, the general pattern was quite similar. The effects of mass flux and quality are addressed in a separate section. The air distribution is reverse of the water distribution. Almost no air flows for the first tube, and the air flow ratio increases to one at fifth tube. Slightly more air is supplied from the twenty-first tube. The variation of air distribution is less significant compared with that of water.

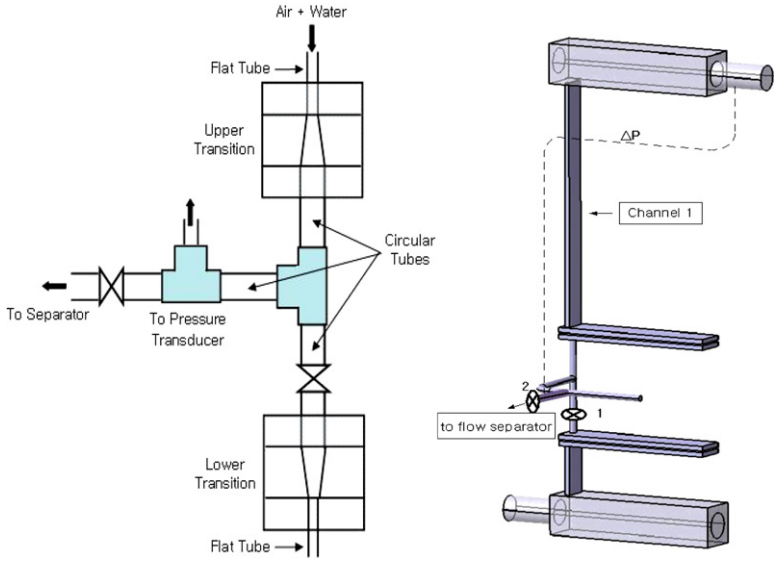

Fig. 5. Schematic drawing illustrating the flow measurement method.

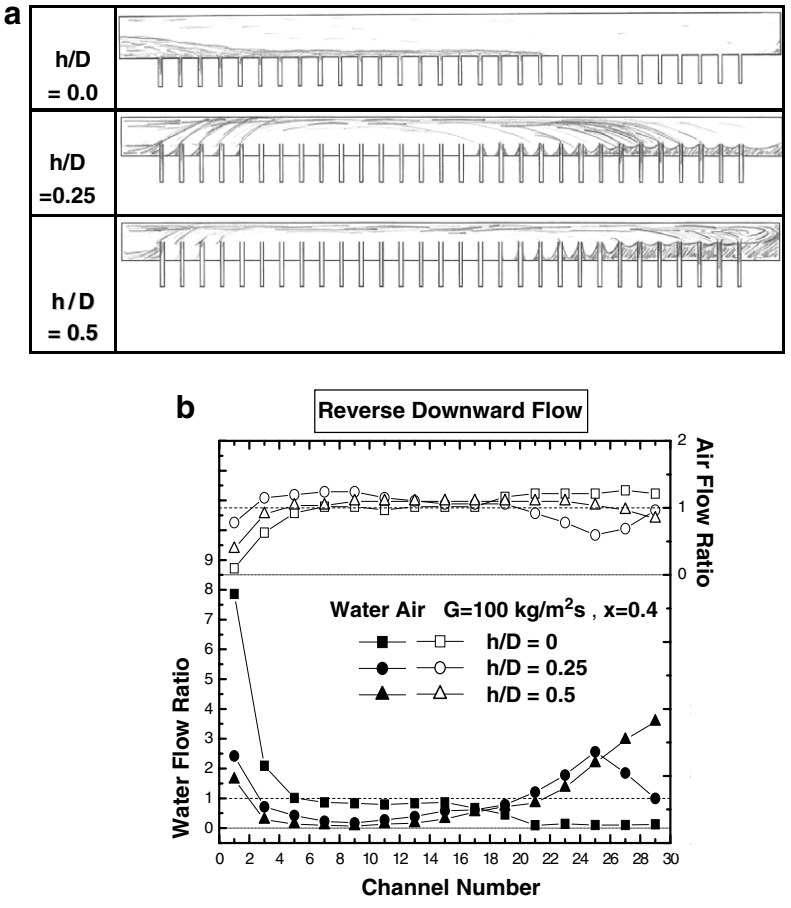

Fig. 6. (a) Typical flow pattern in an upper header with downward flow configuration and (b) corresponding water and air distribution.

With the tube protruded into the header, the flow pattern changes significantly. As shown in the sketch, part of the incoming water impinges at the first protrusion, some of it is sucked in to the first tube, and the remaining water separates at the top, reattaches at the rear part of the header. The water, which bypassed the first protrusion, along with the water from upper part of the header, impinges at the second protrusion, part of it sucked in, separates at the top and reattaches at shorter distance compared with the first protrusion. The process is continued until no water is available. The reattachment length depends on the protrusion depth, mass flux, and quality. As shown in the sketch, the reattachment length increases as the protrusion depth increases. The corresponding data quantifies the effect of protrusion depth. For the protrusion depth to quarter of the header diameter ($h/D = 0.25$), the water flow ratio is 2.5 at the first tube, decreases to the ninth tube, then increases with maximum of 2.7 at twenty-fifth tube, then decreases again. For the protrusion depth to center of the header, the water flow ratio is 1.4 for the first tube, minimum at the fifth tube, and then continuously increases to the end of the header, with maximum 4.0 at the last tube. Thus, we may conclude that as the protrusion increases, more water is forced to rear part of the header with stronger intensity. Similar conclusion has been drawn by Lee and Lee (2004) for a vertical header. The flow pattern sketch of $h/D = 0.5$ further illustrates that, when the reattachment length is larger than the header length, the separated flow hit the rear end of the header, and supplies water from downstream. The air distribution is generally reverse of the water distribution.

The increased protrusion depth of $h/D = 0.5$ will induce larger pressure drop in the header compared with that of the flush-mounted case. The header pressure drop was obtained by subtracting the pressure drop of the last channel from that of the first channel. The channel pressure drop was measured from the inlet of the header to the transition section as illustrated in Fig. 5. The header pressure drop increased as the mass flux, quality, or the protrusion depth increased. At $G = 70$ kg/m^2 s, $x = 0.4$, the header pressure drop was 1.0 kPa for $h/D = 0.0$ and 2.0 kPa for $h/D = 0.5$. At $G = 100$ kg/m^2 s, $x = 0.6$, it increased to 5.9 kPa for $h/D = 0.0$ and to 24.0 kPa for $h/D = 0.5$.

3.1.2. Effect of tube outlet direction

The inlet and the exit may be located at the same side of the heat exchanger (reverse flow), or they may be located at the opposite side of the heat exchanger (parallel flow). Fig. 7 shows the air and water distribution for the reverse flow and the parallel flow configuration for $h/D = 0.5$ at different mass fluxes and qualities. Negligible difference is noticed for the water distribution.

However, the air distributions are significantly different. For the parallel flow, the air flow rate slightly increases or remains the same as the flow travels downstream. For the reverse flow, on the contrary, the air flow rate decreases significantly as the flow travels downstream. This is due to the opposing trend of the header pressure difference between the reverse and the parallel flow as reported by Bajura and Jones (1976). The pressure drop in the header is the sum of the friction and acceleration components. In the upper header, the flow is decelerated due to loss of fluid through branch tubes. This results in a pressure rise, which acts counter to the friction term. However, in the bottom header, the flow accelerates in the flow direction, and the acceleration and friction both contribute to the pressure drop. Therefore, for the reverse flow, the pressure difference across the branch tube decreases as the flow travels downstream. The reverse is true for the parallel flow. Bajura and Jones (1976) showed that, for the single phase flow, the reverse flow yields more uniform flow than the parallel flow. For two-phase flow, however, the flow distribution is affected by additional parameters such as flow regime, quality, etc. Although not shown here, the preceding trends generally apply to other configurations. Thus, succeeding discussions will be provided only for the reverse flow configuration.

3.1.3. Effect of mass flux and quality

Fig. 8 shows the effect of mass flux for different tube protrusion depths. For all the tube protrusion depths, more water flows through the rear part of the header as mass flux increases. For example, for $h/D = 0.5$ at $x = 0.2$ and $G = 70$ kg/m^2 s, the water flow ratio of the first tube is 4.1, decreases to 0.5 at seventh tube, and then increases to maximum 1.5 at nineteenth tube. As the mass flux increases to 100 kg/m^2 s, the water flow ratio of the first tube reduces to 3, and the maximum value of 2.0 is obtained at twenty-third tube. With further increase of mass flux to 200 kg/m^2 s, the water flow ratio of the first tube reduces to 1.1 and the maximum value of 5.2 is obtained at the last tube. This trend is similar to that of the protrusion depth shown in Fig. 6. It appears that as mass flux increases, the reattachment length of the separated flow from the protru-

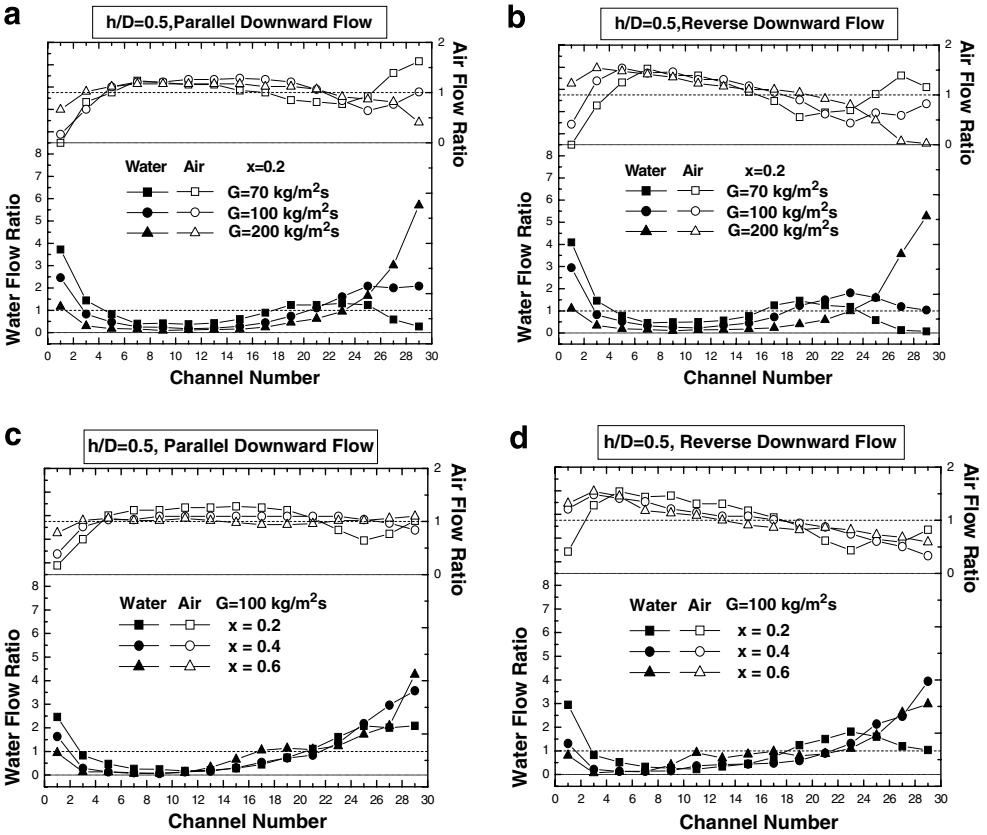

Fig. 7. Graphs showing the effect of tube outlet configuration on water and air distribution for a downward flow configuration: (a) parallel flow ($x = 0.2$), (b) reverse flow ($x = 0.2$), (c) parallel flow ($G = 100$ kg/m^2 s) and (d) reverse flow ($G = 100$ kg/m^2 s).

sion increases due to stronger flow momentum, and the maximum peak moves to downstream of the header with larger magnitude. The air distribution is generally reverse of the water distribution. The same explanation may be provided for $h/D = 0.25$ geometry.

For the flush mounted configuration ($h/D = 0$), at $G = 70$ kg/m^2 s and $x = 0.4$, the water flow ratio of the first tube is 8.2, drastically decreases to 1 at seventh tube, and then continuously decreases to zero at fifteenth tube. With the increase of mass flux to 100 kg/m^2 s, the water flow ratio slight decrease of to 7.9 at the first tube, and almost no flow from the twenty-first tube. With further increase to 130 kg/m^2 s, the water flow ratio is minimum at twenty-third tube, and slightly increases afterwards. It appears that part of the water hits the end of the header and is supplied from downstream. In general, the effect of mass flux is weak compared with that of the protruded configuration. For the flush-mounted configuration, there is no flow distribution mechanism such as separation and reattachment, and only vapor shear will move the liquid to downstream.

Fig. 9 shows the effect of quality for different tube protrusion depths. These graphs are quite similar to Fig. 8. Thus, the same argument as the effect of mass flux may be provided for the effect of quality. As the quality increases, the reattachment length of the separated flow from the protrusions increases due to stronger flow momentum, and the maximum peak moves to downstream of the header with increasing magnitude. Similar to the mass flux case, the effect of quality is not significant for the flush-mounted configuration.

3.2. Upward flow

3.2.1. Flow pattern and tube protrusion effect

Typical flow pattern is illustrated in Fig. 10 along with the water and air distribution data. For all the configurations, most of the water flows through rear part of the header. For flush mounted configuration

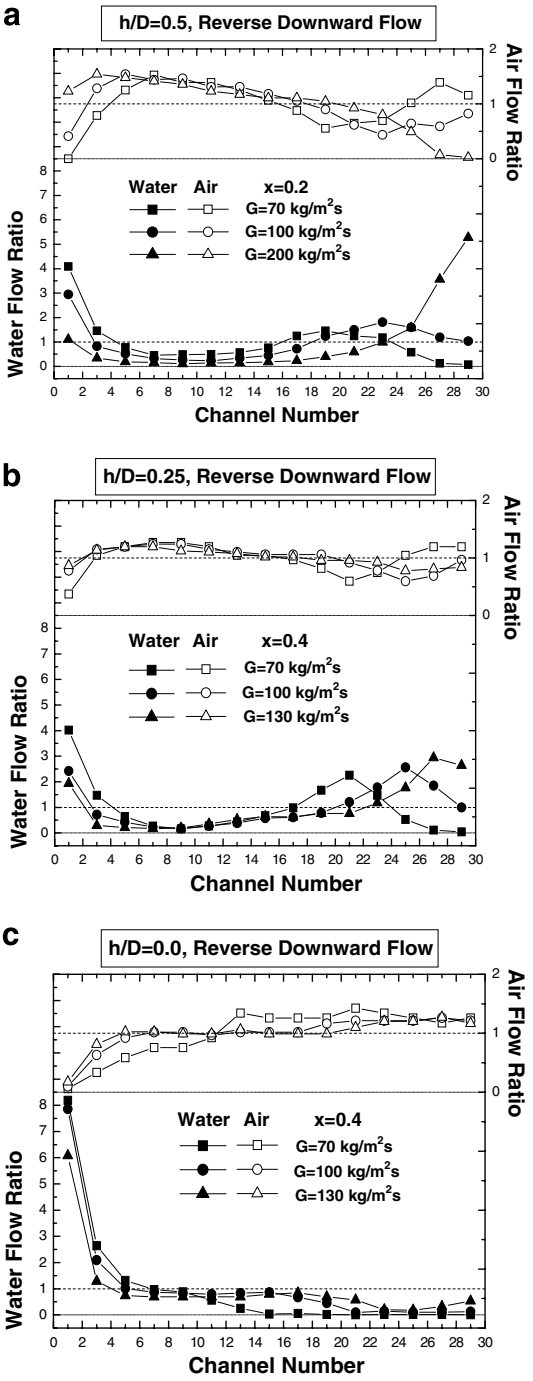

Fig. 8. Effect of mass flux on air and water distribution in the header of downward configuration at $x = 0.4$: (a) $h/D = 0.5$, (b) $h/D = 0.25$ and (c) $h/D = 0.0$.

($h/D = 0$), part of the incoming water flows into the tubes at frontal part of the header. However, most of the water is forced to rear end of the header, and start to fill in the tubes from backward. The data taken at $G = 100$ kg/m^2 s, $x = 0.4$ show that water flow ratio is 1.8 for the first tube, gradually decreases to almost zero at twentieth tube, and then increases reaching 5.3 at the last tube. This pattern was identical independent of

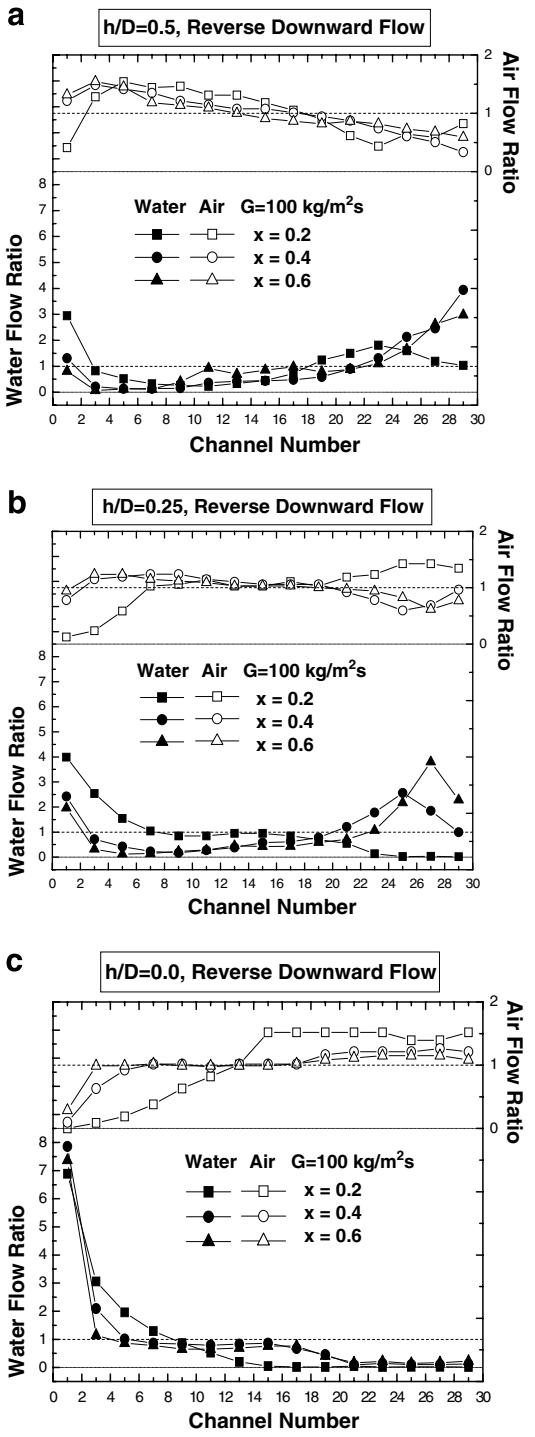

Fig. 9. Effect of quality on air and water distribution in the header of downward configuration at $G = 100\ \mathrm{kg/m^2\,s}$: (a) $h/D = 0.5$, (b) $h/D = 0.25$ and (c) $h/D = 0.0$.

mass flux or quality as long as they are not very low ($G \geqslant 100\ \mathrm{kg/m^2\,s}$ and $x \geqslant 0.4$). The effect of mass flux and quality is addressed in a later section. The air distribution is reverse of the water distribution.

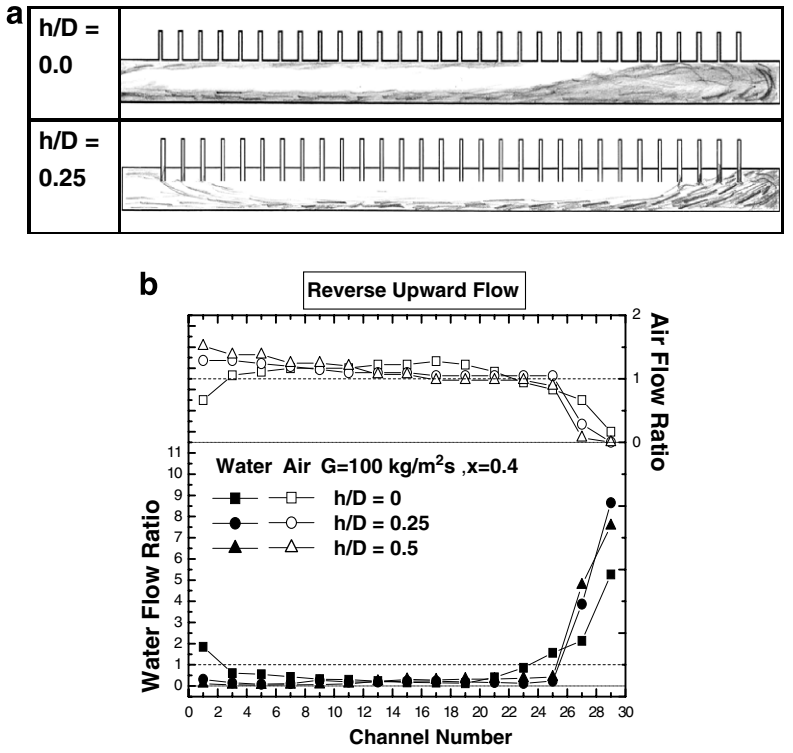

Fig. 10. (a) Typical flow pattern in a lower header with upward flow configuration and (b) corresponding water and air distribution.

With the tube protruded into the header, the flow pattern slightly changes. As shown in the sketch, part of the incoming water impinges at the first protrusion, separates at the top, reattaches at the bottom of the header due to the action of gravity. The separated water, along with the water from lower part of the header, is forced to the rear end of the header, and starts to fill in the tubes from backward. The data taken at $G = 100$ kg/m^2 s, $x = 0.4$ show that almost no water is supplied until twenty-sixth tube, and the water flow ratio drastically increases afterwards. The protrusion depth does not significantly affect the flow pattern. For the upward configuration, the separated water from the upper protrusions reattach at the bottom of the header. In this case, the variation of the reattachment length caused by the change of protrusion depth will not significantly affect the flow distribution. The same argument may also apply to the effect of mass flux or quality.

Similar to the downward flow, the header pressure drop increased as the mass flux, quality, or the protrusion depth increased. However, the magnitude was smaller. At $G = 70$ kg/m^2 s, $x = 0.4$, the header pressure drop was 0.5 kPa both for $h/D = 0.0$ and $h/D = 0.5$. At $G = 100$ kg/m^2 s, $x = 0.6$, it increased to 3.6 kPa for $h/D = 0.0$ and 17.5 kPa for $h/D = 0.5$.

3.2.2. Effect of tube outlet direction

Similar to the downward flow, negligible difference in the water distribution was noticed between the reverse flow and the parallel flow. Even the air distributions were approximately the same. For the downward flow, the air distributions between the reverse and the parallel flow were quite different, and the difference was explained following Bajura and Jones (1976). The Bajura and Jones argument applies to single phase flow. For two-phase flow, the flow distribution is affected by additional parameters such as flow regime, quality, etc. Succeeding discussions will be provided for the reverse flow configuration.

3.2.3. Effect of mass flux and quality

Fig. 11 shows the effect of mass flux for different tube protrusion depths at $x = 0.4$. For all tube protrusion depths, the mass flux does not significantly affect the water or air distribution for $G \geqslant 100$ kg/m^2 s (although a

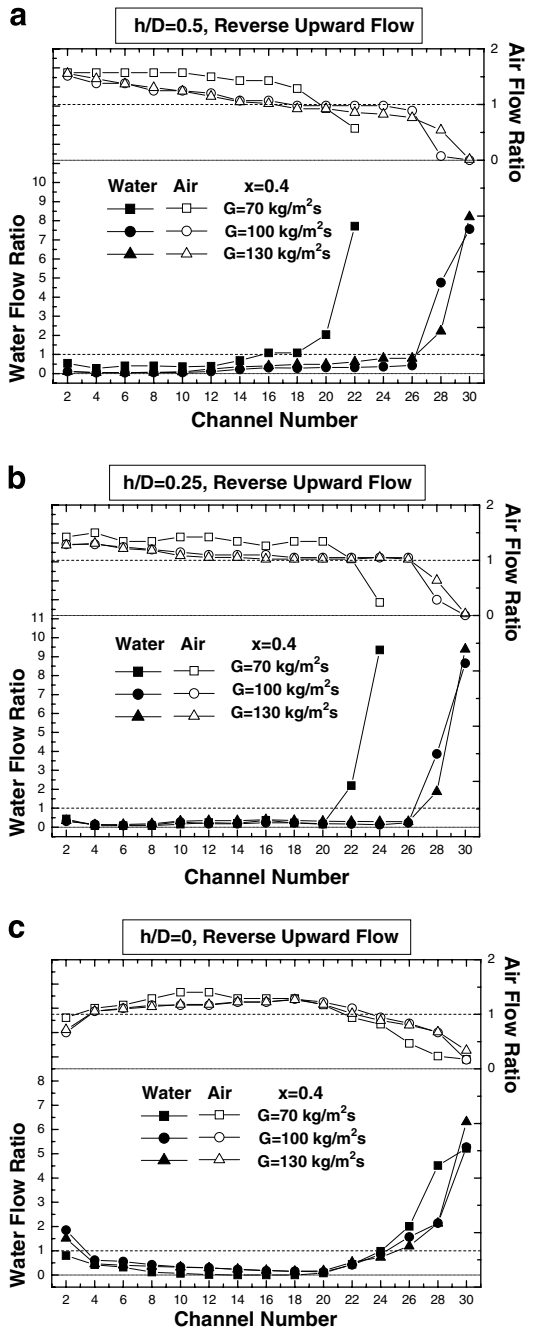

Fig. 11. Effect of mass flux on air and water distribution in the header of upward configuration at $x = 0.4$: (a) $h/D = 0.5$, (b) $h/D = 0.25$ and (c) $h/D = 0.0$.

stronger push of water is noticed at the rear part of the header at higher mass flux). At $G = 70$ kg/m^2 s, however, no data was obtained at the rear part of the header. A stagnant water region formed at the rear part of the upper header, where virtually no water or air flow was observed. In this case, maximum water flow was obtained at the tube located just upstream of the stagnant region. For the reverse flow configuration, the pressure difference across the tube is minimum at the last tube, according to Bajura and Jones (1976). If the pressure difference is less than the hydraulic head needed to push the water through the tube, no flow will be

formed. It appears that, at the low mass flux, the pressure difference at the rear part of the header is not sufficient to push the water through the tubes. As the mass flux increased, the stagnant region disappeared. Fig. 11c shows that no stagnant region exists for the flush-mounted configuration.

Fig. 12 shows the effect of quality for different tube protrusion depths. These graphs are quite similar to Fig. 11. Thus, the same argument may be provided for the effect of quality. Except for the low quality ($x = 0.2$), the quality does not significantly affect the water or air distribution for $x \geqslant 0.4$ (although a stronger

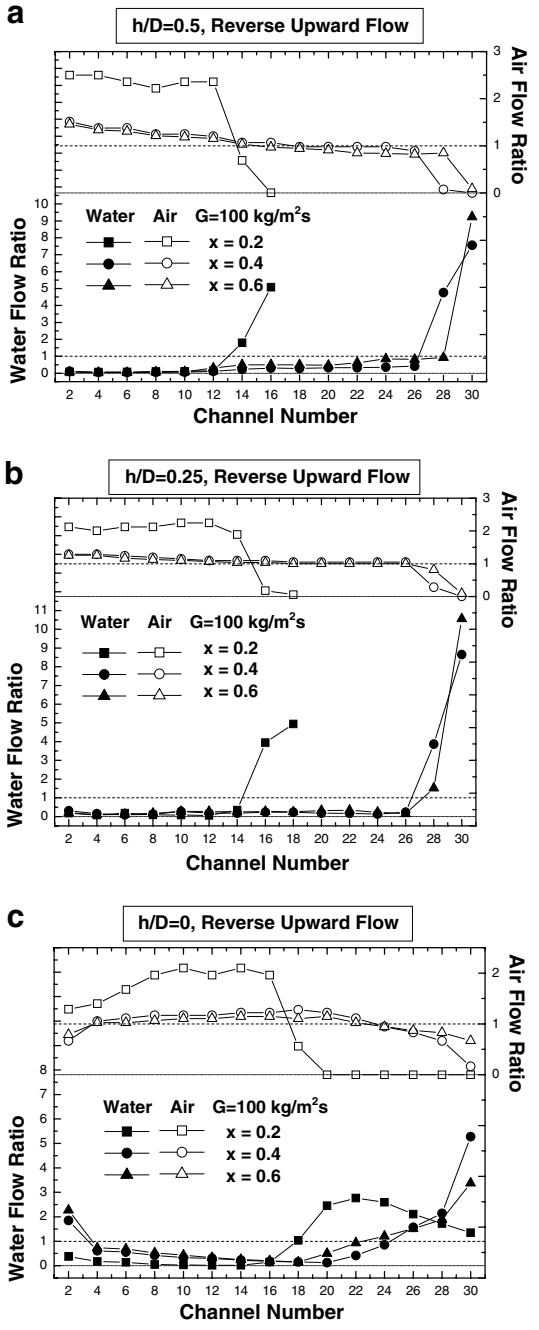

Fig. 12. Effect of quality on air and water distribution in the header of upward configuration at $G = 100\ \mathrm{kg/m^2\,s}$: (a) $h/D = 0.5$, (b) $h/D = 0.25$ and (c) $h/D = 0.0$.

push of water is noticed at the rear part of the header at higher quality). At $x = 0.2$, stagnant water region forms at the rear part of the upper header, and no flow is observed. The stagnant region disappears at higher quality. Fig. 12c shows that no stagnant region exists at $h/D = 0$.

4. Recommended future work

The effects of flow direction, tube outlet direction and the protrusion depth on the air–water two-phase distribution were investigated in this study for a horizontal header having 30 vertical flat tubes. The flow pattern at the header inlet was annular. The density ratio of the present air–water is 0.0012, which is much smaller than that of typical refrigerant. For example, the density ratio of R-134a at 0 °C is 0.011, which is approximately nine times larger than that of air–water. Then, the flow pattern in the header of an actual evaporator could be different from the present annular flow. The header diameter, header shape as well as the mass flux or quality will also affect the flow pattern.

The header length (or the number of tubes) per pass may also affect the flow distribution. The present results show that, for downward flow, the reattachment length of the separated flow from frontal tubes is a key factor affecting the flow distribution in the header. If the header is shorter than the reattachment length, the separated flow hits the far end of the header, and supplies the liquid from backward. In such case, more uniform flow distribution will result. For upward flow, however, the reattachment length did not significantly affect the flow distribution, which will also hold for shorter header. The header inlet orientation will also affect the flow distribution. Most of the actual inlets are normal to the header. Future researches on these subjects are recommended.

5. Conclusions

In this study, the air and water flow distribution are experimentally studied for a heat exchanger composed of horizontal round headers and vertical 30 flat tubes. The effects of tube outlet direction, tube protrusion depth as well as mass flux, and quality are investigated. The flow at the header inlet is annular. For the downward flow configuration, the water flow distribution is significantly affected by the tube protrusion depth. For flush-mounted configuration, most of the water flows through frontal part of the header. As the protrusion depth increases, more water is forced to the rear part of the header. It is observed that the incoming water impinges at the protrusions, and the separated water reattaches at the rear part of the header. The reattachment length increases as the protrusion depth increases. The effect of mass flux or quality is qualitatively the same as that of the protrusion depth. Increase of the mass flux or quality forces the water to rear part of the header. For the upward flow configuration, most of the water flows through the rear part of the header. The protrusion depth, mass flux, or quality does not significantly alter the flow distribution. Different from the downward flow configuration, the separated water from upper protrusions reattaches at the bottom of the header. Thus, the variation of reattachment length by the change of protrusion depth, mass flux or quality is not like to significantly affect the flow distribution. Negligible difference on the water flow distribution was observed between the parallel flow and the reverse flow configuration.

Acknowledgement

The funding of this research was provided by KOSEF (R05-2003-000-10170).

References

Bajura, R.A., Jones, E.H., 1976. Flow distribution in manifolds. J. Fluids Eng. 98, 654–666.

Bernoux, P., Mercier, P., Lebouche, M., 2001. Two-phase flow distribution in a compact heat exchanger. In: Proc. 3rd Int. Conf. Compact Heat Exchangers, pp. 347–352.

Bullard, C.W., 2002. Design tradeoffs in microchannel heat exchangers, ACRC Report #124.

Cho, H., Cho, K., Kim, Y., 2003. Mass flow rate distribution and phase separation of R-22 in multi-microchannel tubes under adiabatic condition. In: 1st Int. Conf. Microchannels and Minichannels, pp. 527–533.

Hrnjak, P., 2004. Flow distribution issues in parallel flow heat exchangers. ASHRAE Annual Meeting, AN-04-1-2.

Lee, J.K., Lee, S.Y., 2004. Distribution of two-phase annular flow at header-channel junctions. Exp. Therm. Fluid Sci. 28, 217–222.
Rong, X., Kawaji, M., Burgers, J.G., 1995. Two-phase header flow distribution in a stacked plate heat exchanger. Gas Liquid Flows Fed-Vol. 225, 115–215.
Tompkins, D.M., Yoo, T., Hrnjak, P., Newell, T., Cho, K., 2002. Flow distribution and pressure drop in micro channel manifolds. In: 9th Int. Refrigeration and Air Conditioning Conference at Purdue, R6-4.
Vist, S., Pettersen, J., 2004. Two-phase flow distribution in compact heat exchanger manifolds. Exp. Thermal Fluid Sci. 28, 209–215.
Watanabe, M., Katsuda, M., Nagata, K., 1995. Two-phase flow distribution in multi-pass tube modeling serpentine type evaporator. ASME/JSME Thermal Eng. Conf. 2, 35–42.
Webb, R.L., Chung, K., 2004. Two-phase flow distribution in tubes of parallel flow heat exchangers. Heat Transfer Eng. 26, 3–18.